

# Is it reasonable to assume a uniformly distributed cooling-rate along the microslide of a directional solidification stage?

Y. RABIN

*Department of Mechanical Engineering, Technion – Israel Institute of Technology, Haifa 32000, Israel*

**Key words.** Cooling-rate, cryostage, directional solidification, temperature distribution, thermal analysis,

## Summary

It is commonly assumed that the cooling-rate along the microslide of a directional solidification stage is uniformly distributed, an assumption which is typically applied in low cooling-rates studies. A new directional solidification stage has recently been presented, which is specified to achieve high cooling-rates of up to  $1.8 \times 10^4 \text{ }^\circ\text{C min}^{-1}$ , where cooling-rates are still assumed to be uniformly distributed. The current study presents a closed-form solution to the temperature distribution and to the cooling-rate in the microslide. Thermal analysis shows that the cooling-rate is by no means uniformly distributed and can vary by several hundred percent along the microslide in some cases. Therefore, the mathematical solution presented in this study is essential for experimental planning of high cooling-rate experiments.

## Introduction

The mechanisms of cell injury during freezing are of great interest in the study of cryobiology. Analysis of the freezing process can be performed in real time, by placing the biological specimen on a temperature-controlled stage (also termed cryostage) and, consequently, controlling the thermal history of the specimen. Cryostage applications have been reported for more than four decades, based on two major controlling techniques: (i) by time-controlling of a cryostage possessing a uniform temperature distribution (Luyet & Rapatz, 1957; Diller & Cravalho, 1971; Diller, 1982; Cosman *et al.*, 1989); and (ii) by sliding a microslide, carrying a biological specimen, at a controlled velocity, between two temperature-controlled bases (also known as a

directional solidification stage) (Brower *et al.*, 1981; Korber *et al.*, 1983; Rubinsky & Ikeda, 1985; Rubinsky *et al.*, 1993; Namperumal & Coger, 1998; Tatsutani & Rubinsky, 1998).

Diller & Cravalho (1971) noted that cooling-rates in the wide spectrum of  $1 \text{ }^\circ\text{C min}^{-1}$  to  $10^4 \text{ }^\circ\text{C min}^{-1}$  are of interest in the study of cryobiology. Nevertheless, most of the reported directional solidification studies address the lower range of the cooling-rate spectrum, up to the order of  $10^1 \text{ }^\circ\text{C min}^{-1}$ . Microslide velocities of up to the order of  $10^2 \text{ } \mu\text{m s}^{-1}$  are typically applied in driving these low cooling-rates. Under these conditions, and when ignoring the transliteration effect of the microslide, the temperature distribution between the temperature bases is assumed to be linear and, hence, the cooling-rate is assumed to be uniformly distributed (Rubinsky & Ikeda, 1985). A new directional solidification stage has been presented recently by Namperumal & Coger (1998), which is specified to achieve cooling-rates of up to  $1.8 \times 10^4 \text{ }^\circ\text{C min}^{-1}$ . In their report, Namperumal and Coger assume that the temperature and the cooling-rate distributions have the same characteristics as in the cases of low cooling-rates.

The current study focuses on thermal analysis of heat transfer in the microslide. This study provides insight with regard to the conditions under which it is reasonable to assume a linear temperature distribution along the microslide and a uniformly distributed cooling-rate, assumptions which significantly affect experimental planning.

## Mathematical formulation

### *The approximate solution*

Specific designs of directional solidification stages are available in the literature (Brower *et al.*, 1981; Korber *et al.*, 1983; Rubinsky & Ikeda, 1985; Tatsutani & Rubinsky, 1998; Namperumal & Coger, 1998). Figure 1 illustrates the

Correspondence to: Dr Yoed Rabin, Carnegie Mellon University, Pittsburgh, PA 15213, U.S.A. Tel: + 1 412 268 3488; e-mail: yoed.rabin@andrew.cmu.edu

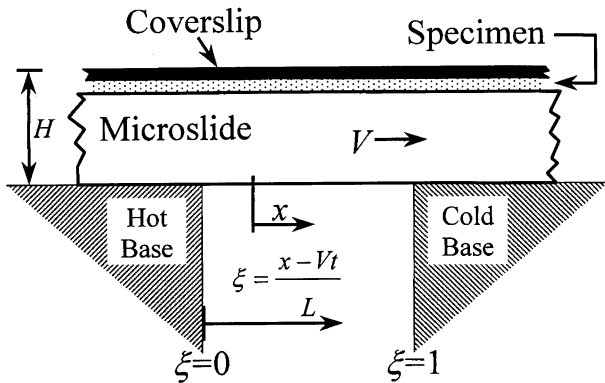


Fig. 1. Schematic illustration of the microslide, the hot and cold bases, and the coordinate systems used for the thermal analysis, where the origin of coordinate  $x$  moves with the microslide at a constant velocity  $V$  and the coordinate  $\xi$  is stationary and normalized by the distance between the temperature bases,  $L$ .

major components of a directional solidification stage. The coordinate  $x$  indicates the direction of sliding from the hot base to the cold base, while the coordinate origin moves with the microslide at a constant velocity  $V$  relative to the temperature bases. It is customary to assume that the temperature distribution varies linearly between the temperature bases, and that the microslide experiences uniform cooling at a rate of:

$$\frac{dT}{dt} = -V \frac{(T_h - T_c)}{L} \quad (1)$$

where  $T$  is the microslide temperature,  $T_h$  is the hot base temperature,  $T_c$  is the cold base temperature,  $t$  is the time and  $L$  is the distance between the temperature bases. The purpose of the following thermal analysis is to show that Eq. (1) is not adequate for the general case of heat transfer within the microslide, but can serve as an approximation for some specific cases. Hence, Eq. (1) is defined as the approximate solution in this study.

### Mathematical modelling

Both the microslide and the coverslip are made of glass, where the thickness of the specimen layer is negligible compared to the thickness of the microslide. The width of the microslide is typically of an order of magnitude larger than the thickness of the microslide. Hence, for simplicity, it is assumed that the heat transfer prevails solely in a glassy plate (microslide) having a thickness  $H$ , which equals the sum of the microslide thickness and the coverslip thickness (Fig. 1). It is further assumed that the temperature is uniformly distributed at any given cross-section perpendicular to  $x$ . Under these conditions, the microslide can be modelled as a thermal fin (Carslaw

& Jaeger, 1959):

$$\frac{\partial^2 T}{\partial x^2} - \frac{2h}{kH}(T - T_\infty) = \frac{1}{\alpha} \frac{\partial T}{\partial t} \quad (2)$$

where  $h$  is the combined heat transfer coefficient by convection and radiation to the surroundings,  $k$  is the thermal conductivity of glass (is the thermal diffusivity of glass,  $H$  is the thickness and  $T_\infty$  is the surrounding temperature.

The assumption of a uniform temperature distribution perpendicular to  $x$  is known to be valid for low Biot number only, where Biot number is defined as:

$$Bi = \frac{hH}{k} \quad (3)$$

Typical values of  $h$ ,  $H$  and  $k$  are  $10 \text{ W m}^{-2} \text{ }^\circ\text{C}^{-1}$ ,  $1 \text{ mm}$  and  $0.78 \text{ W m}^{-2} \text{ }^\circ\text{C}^{-1}$ , respectively. These values yield a  $Bi$  value of the order of  $10^{-2}$ , which justifies the assumption of a uniform temperature in the cross-section perpendicular to  $x$ .

Because the boundary conditions of the heat transfer problem in  $x$  are time-dependent, it is most convenient to transform the heat transfer problem by using a normalized and stationary coordinate (Fig. 1) in combination with the following dimensionless temperature and time:

$$\xi = \frac{x - Vt}{L}; \quad \theta = \frac{T_h - T}{T_h - T_c}; \quad Fo = \frac{\alpha t}{L^2} \quad (4)$$

where  $Fo$  is known as the Fourier number. Using these definitions, Eq. (2) is transformed to the following dimensionless form:

$$\frac{\partial^2 \theta}{\partial \xi^2} + a \frac{\partial \theta}{\partial \xi} + b(\theta - \theta_\infty) = \frac{\partial \theta}{\partial Fo} \quad (5)$$

where

$$a = \frac{VL}{\alpha}; \quad b = -\frac{2hL^2}{kH} \quad (6)$$

It follows that the boundary conditions of Eq. (5) are  $\theta(0) = 0$  and  $\theta(1) = 1$ .

### The exact solution

Equation (5) is a parabolic equation with constant parameters and constant boundary conditions and therefore is expected to reach steady-state in  $\xi$ , which is a quasi-steady condition in  $x$ . The steady-state solution is addressed first, and the time period beyond which a steady-state can be assumed is addressed below in the results and discussion section. The time-dependent term of Eq. (5) vanishes at steady-state and its solution is:

$$\theta(\xi, t = \infty) = \theta_\infty + \frac{1}{(e^\gamma - 1)} \left\{ \theta \left[ e^{0.5\xi(\gamma-a)} - e^{\gamma-0.5\xi(\gamma+a)} \right] + (1 - \theta_\infty) \left[ e^{0.5\xi(\gamma-a)+0.5(\gamma+a)} - e^{0.5(1-\xi)(\gamma+a)} \right] \right\} \quad (7)$$

where  $\gamma^2 = a^2 - 4b$ .

**Table 1.** Typical thermophysical properties and parameters.

Microslide velocity, $V$	0–500 $\mu\text{m s}^{-1}$
Microslide thickness, $H$	1 mm
Distance between temperature bases, $L$	0.5 mm to 3.2 mm
Hot base temperature, $T_h$	60 °C to 150 °C
Cold base temperature, $T_c$	– 60 °C to – 150 °C
Surrounding temperature, $T_\alpha$	$\approx$ 20 °C
Thermal conductivity of glass at room temperature, $k$	0.78 $\text{W m}^{-1} \text{ }^\circ\text{C}^{-1}$
Thermal diffusivity of glass at room temperature, $\alpha$	$3.4 \times 10^{-7} \text{ m}^2 \text{ s}^{-1}$
Heat transfer coefficient by convection and radiation, $h$	10 $\text{W m}^{-2} \text{ }^\circ\text{C}^{-1}$

The quasi-steady cooling-rate can now be calculated as follows:

$$\begin{aligned}
 \frac{\partial T}{\partial t} &= -\frac{V}{L} \frac{\partial T}{\partial \xi} = -V \frac{(T_h - T_c)}{L} \frac{\partial \theta}{\partial \xi} \\
 &= -V \frac{(T_h - T_c)}{L} \frac{0.5}{(e^\gamma - 1)} \\
 &\times \left\{ \theta_\infty [(\gamma - a)e^{0.5\xi(\gamma-a)} + (\gamma + a)e^{\gamma-0.5\xi(\gamma+a)}] \right. \\
 &+ (1 - \theta_\infty) \\
 &\times \left. [(\gamma - a)e^{0.5\xi(\gamma-a) + 0.5(\gamma+a)} + (\gamma + a)e^{0.5(1-\xi)(\gamma+a)}] \right\}
 \end{aligned} \quad (8)$$

Equation (8) is defined as the exact solution for the cooling-rate in the current study. Comparing the third term from left of Eq. (8) with Eq. (1), one can see that the value  $\partial\theta/\partial\xi$  is

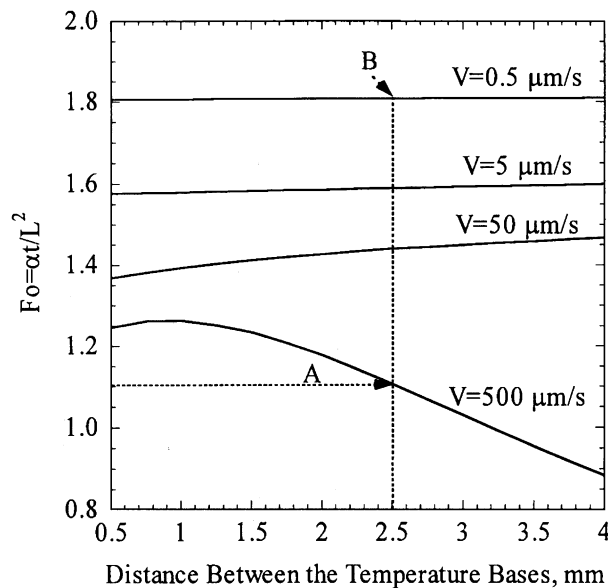


**Fig. 2.** Dimensionless time parameter  $Fo$  beyond which steady-state heat transfer may be assumed in the microslide.

actually the ratio of the exact cooling-rate to the approximate cooling-rate. This ratio indicates the deviation of the exact cooling-rate from the approximate one.

## Results and discussion

A very wide cooling-rate spectrum, typically from  $1 \text{ }^\circ\text{C min}^{-1}$  to  $10^4 \text{ }^\circ\text{C min}^{-1}$ , is of interest in the study of cryobiology. Rubinsky & Ikeda (1985) have suggested that a cryostage comprises a hot base temperature of up to +60 °C, a cold base temperature of down to –60 °C, a distance between the temperature bases of 3.2 mm, and a varying microslide velocity. The cryostage built by Rubinsky and Ikeda has proved to be simple, versatile and accurate in controlling the temperatures. In order to achieve higher cooling-rates, Namperumal & Coger (1998) have suggested a modified device, having a hot base temperature of up to +150 °C, a cold base temperature of down to –150 °C, a varying distance between the temperature bases in the range 0.5 mm to 2.5 mm, and a varying microslide velocity in the range  $5 \text{ } \mu\text{m s}^{-1}$  to  $500 \text{ } \mu\text{m s}^{-1}$ . Based on the approximate solution, Eq. (1), Namperumal and Coger have predicted that their cryostage is capable of achieving uniformly distributed cooling-rates of up to  $1.8 \times 10^{-4} \text{ }^\circ\text{C min}^{-1}$ .

Based on these specifications, and unless otherwise specified, the current thermal analysis applies the following parameters: a fixed hot base temperature of +37 °C, a fixed cold base temperature of –150 °C, a varying microslide velocity in the range  $0.5 \text{ } \mu\text{m s}^{-1}$  to  $400 \text{ } \mu\text{m s}^{-1}$ , and a varying distance between the hot and cold bases in the range 0.5 mm to 4 mm. Although higher temperatures of the hot base are achievable, it is assumed that the biological material will severely deteriorate if exposed to temperatures above +37 °C for long periods. Nevertheless, the effect of using higher hot base temperatures on the outcome of the parametric study is addressed below. Other thermophysical properties and experimental parameters applied in this study are listed in Table 1.

### Time to steady-state

The exact solution is applicable for steady-state only, a

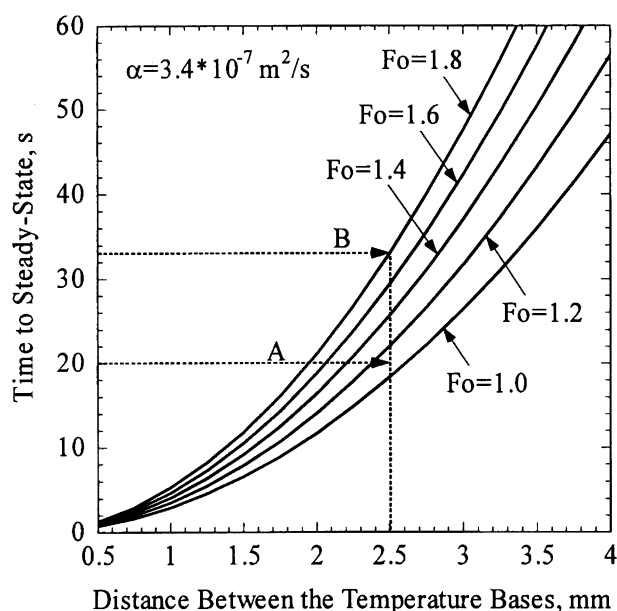


Fig. 3. Time period between the initiation of the microslide movement and steady-state.

condition which enables experimentation under constant conditions. In order to find the time period from the initiation of the microslide movement to steady-state, a transient numerical solution of the governing equation, Eq. (5), has been compared with the exact and steady-state solution, Eqs. (6)–(8). For practical purposes, a cooling-rate difference of less than 1% between the numerical solution and the steady-state (exact) solution was deemed sufficient to define the beginning of steady-state. The numerical solution was based on the Crank-Nicolson technique (Carnahan *et al.*, 1969), which is an unconditionally stable finite-differences scheme. Accordingly, Fig. 2 shows the dimensionless time parameter  $Fo$  beyond which steady-state may be assumed. It was found numerically that a cooling-rate difference of less than 1% leads to a temperature distribution difference of less than 0.4% between the numerical and exact solutions.

Figure 3 shows the actual time in seconds from the initiation of the microslide movement to steady-state for various  $Fo$  values. For example,  $Fo$  values of about 1.1 and 1.8 are required for microslide velocities of  $500 \mu\text{m s}^{-1}$  and  $0.5 \mu\text{m s}^{-1}$ , respectively, and for a distance of 2.5 mm between the temperature bases (points A and B in Fig. 2, respectively). These  $Fo$  values lead to actual time periods of 20 s and 33 s, respectively (points A and B in Fig. 3, respectively), until steady-state may be assumed. The microslide moves 10 mm in 20 s at a velocity of  $500 \mu\text{m s}^{-1}$ , which is a significant distance and must be taken into account in the experimental planning. The travelling distance in 33 s at a velocity of  $0.5 \mu\text{m s}^{-1}$  is not significant, but this time must be taken into account in

experimental planning. In all cases, the cooling-rates are significantly higher at the initiation period, prior to steady-state.

#### Steady-state temperature distribution and cooling-rate

Figure 4 shows the exact temperature distribution (solid lines) and the approximate temperature distribution (dashed lines) at steady-state. It can be seen that the temperature distribution deviates significantly from the commonly accepted linear approximation at higher velocities. Figure 5 shows the cooling-rate ratio of the exact solution, Eq. (8), to the approximate solution, Eq. (1). As discussed above, this cooling-rate ratio is equal to  $\partial\theta/\partial\xi$ . It can be seen from Fig. 5 that the cooling-rate is by no means uniformly distributed along the microslide at steady-state.

At high velocities, say higher than  $25 \mu\text{m s}^{-1}$ , the maximal cooling-rate is found near the hot base and decreases from the hot to the cold base. At a velocity of  $400 \mu\text{m s}^{-1}$  for example (Fig. 5a), this ratio varies from 4 near the hot base down to 0.2 near the cold base. At lower velocities, say lower than  $5 \mu\text{m s}^{-1}$ , the cooling-rate distribution increases monotonically from the hot to the cold base. The reason for this difference in thermal behaviour is that the parameter  $a$  of Eq. (5) is more significant than the parameter  $b$  at higher velocities, and vice versa at lower velocities. The physical meaning of this is that the heat transfer to the surroundings dominates the cooling-rate distribution at low velocities. Overall, the exact cooling-rate deviates from the approximate cooling-rate in a range of  $-5\%$  to  $+10\%$  for microslide velocities of less than  $25 \mu\text{m s}^{-1}$ . A more careful analysis is in order for higher velocity experiments, as is demonstrated below.

#### Numerical example of high velocity

Let us assume that a cooling-rate of  $900 \text{ }^\circ\text{C min}^{-1}$  at  $-0.4 \text{ }^\circ\text{C}$  is of interest for a specific case study. Let us further assume that this study is planned according to the approximate solution as follows: a hot base temperature of  $+37 \text{ }^\circ\text{C}$ , a cold base temperature of  $-150 \text{ }^\circ\text{C}$ , a distance of 2.5 mm, and a microslide velocity of  $200 \mu\text{m s}^{-1}$ . For this case, the temperature distribution and the cooling-rate ratio are shown in Figs 4b and 5b, respectively. The value of  $\theta$  for this case is 0.2, Eq. (4), and the value of  $\xi = 0.2$  is estimated according to the approximate solution (following the dashed line in Fig. 4b, where A is the approximated working point). This means that a cooling-rate of  $900 \text{ }^\circ\text{C min}^{-1}$  at  $-0.4 \text{ }^\circ\text{C}$  is approximated at a distance of 0.5 mm from the hot base. However, the exact solution indicates that the non-dimensional temperature at this point is 0.324 (point B in Fig. 4b), which leads to an actual working temperature of  $-23.6 \text{ }^\circ\text{C}$  at the same point. Assuming that biological solutions have similar thermal

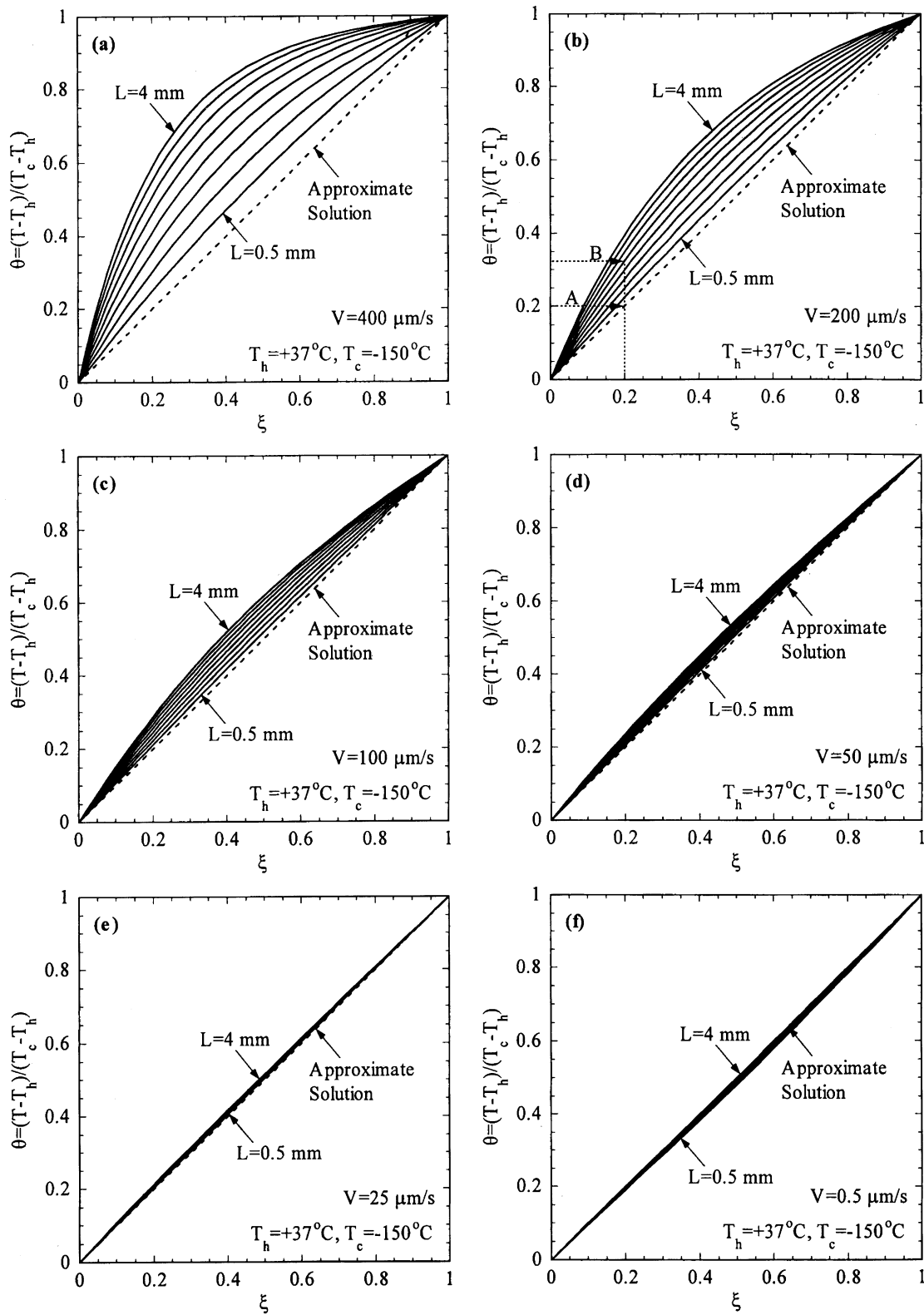


Fig. 4. Exact temperature distribution for distances between the temperature bases in the range 0.5 mm to 4 mm, shown every 0.5 mm increment (solid lines), and the approximate temperature distribution (dashed line).

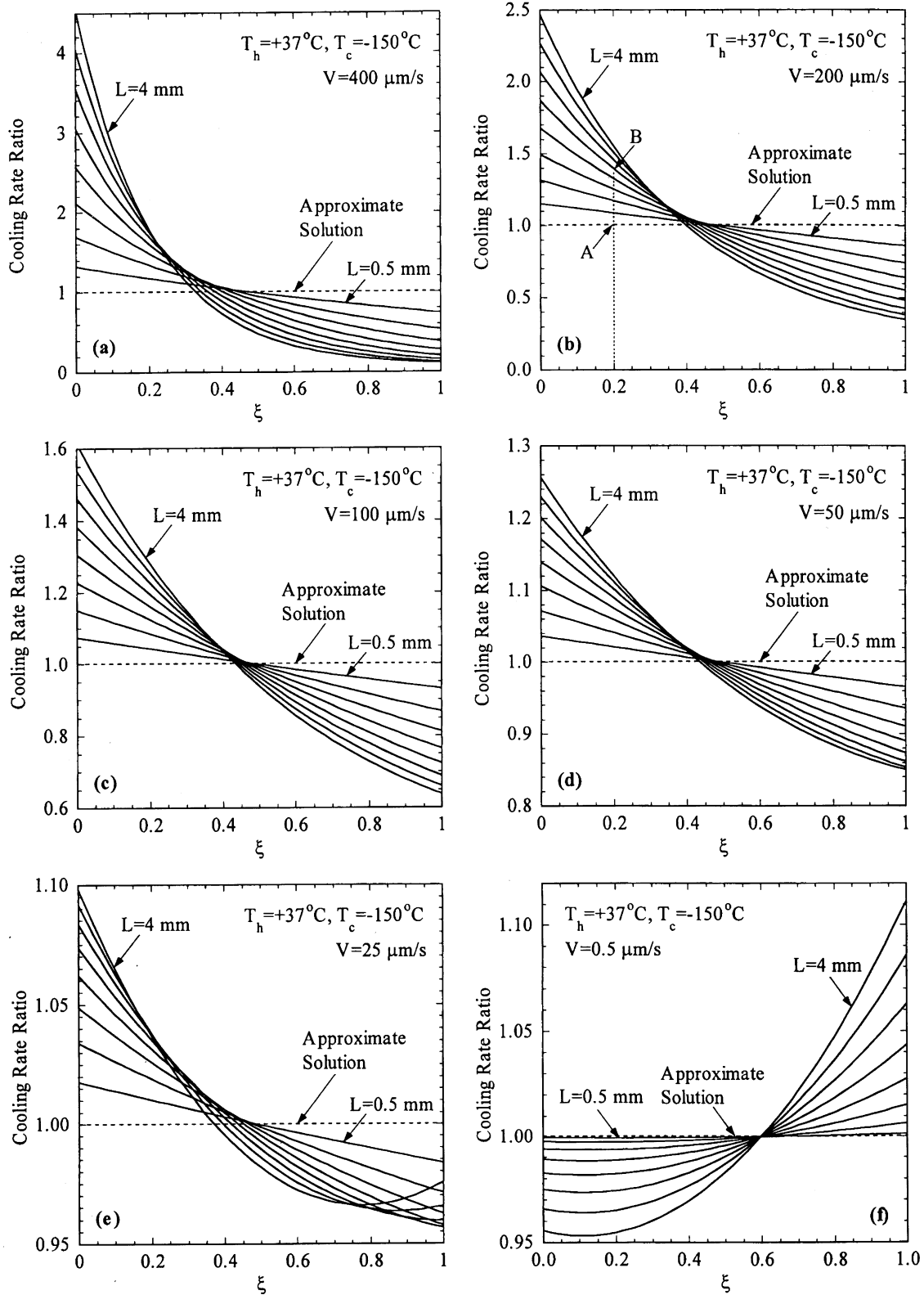


Fig. 5. Cooling rate ratio of the exact solution to the approximate solution for distances between the temperature bases in the range 0.5 mm to 4 mm, shown every 0.5 mm increment.

behaviour to NaCl solution, and taking into account that pure water freezes at 0 °C, while the eutectic point of NaCl solution is -22 °C, the above overestimation of the temperature, of 23.2 °C at the point of observation, may dramatically affect the analysis of this particular experiment.

Figure 5b shows a cooling-rate ratio of 1.4 at the same point of observation (point B in Fig. 5b), which means an actual cooling-rate of 1260 °C min<sup>-1</sup> rather than the approximated cooling-rate of 900 °C min<sup>-1</sup>. Furthermore, the point of observation experiences a cooling-rate of 1680 °C min<sup>-1</sup>, as it leaves the hot base, which decreases monotonically as it approaches the point of observation. This may have a further effect on the process of freezing.

Clearly, the approximate solution is completely inadequate for this case study. Furthermore, the above numerical example addresses an approximated cooling-rate which is only 5% of the maximal predicted cooling-rate for the cryostage suggested by Namperumal & Coger (1998).

One way of improving the results of the above case study is by decreasing the distance between the temperature bases and, consequently, decreasing the microslide velocity. Taking the distance of 1 mm, a microslide velocity of 80 µm s<sup>-1</sup> is required to maintain the same approximated cooling-rate of 900 °C min<sup>-1</sup>. The exact temperature and exact cooling-rate in this modified case are -3.9 °C and 960 °C min<sup>-1</sup>, respectively, at the same working point. Clearly, both the microslide velocity and the distance have major effects upon the correlation between the exact and approximate solutions.

An alternative way of forcing a constant cooling-rate, within the high cooling-rate part of the spectrum, is by applying a varying microslide velocity. However, the pre-specified cooling-rate relates to a pre-specified location on the microslide and not to the entire area of the microslide. Furthermore, the exact solution presented in this work will not be applicable in this case, and the heat transfer problem should be solved numerically.

#### *The effect of the temperature gradient*

It appears that the minimal distance always leads to a better agreement between the approximate and the exact solutions. By contrast, the temperature gradient between the temperature bases increases with the decrease in the distance between the temperature bases. In general, the temperature gradient for a distance of 0.5 mm is about five times the temperature gradient for a distance of 2.5 mm, when all the other experimental parameters are held constant. At low velocities, a very reasonable uncertainty of 0.05 mm in the actual location of observation between the temperature bases leads to an uncertainty of 18.5 °C and 3.7 °C in the actual temperature at the same point, for distances of 0.5 mm and 2.5 mm,

respectively. This uncertainty increases dramatically at high velocities. Note that temperature measurements in a resolution of 0.05 mm using standard temperature sensors are not feasible.

An alternative for calibration of the microslide temperature has been suggested by Tatsutani & Rubinsky (1998), by attaching capillaries containing saline of various concentrations. Each solution freezes at a different specific temperature according to its concentration and, hence, acts as a temperature indicator. However, due to the dynamics of freezing, this alternative is expected to be accurate only at low cooling rates.

#### *The effect of base temperature*

Figures 4 and 5 are given as representative results, which are presented for a hot base temperature of +37 °C and a cold base temperature of -150 °C. Although not presented here, all the cases shown in Figs 4 and 5 were redrawn for a hot base temperature of +150 °C, but no significant changes were found between these two general cases, when the results were presented in a non-dimensional form. The only source of disagreement between the two general cases is the value of the production of  $b$  and  $\theta_\infty$  in Eq. (5), where the values of  $b$  and  $\theta_\infty$  are typically less than 0.2 and 0.5, respectively. The value of this production is significant at low velocities only, where the parameter  $a$  may be of the same order of magnitude as  $b\theta_\infty$ . However, in general, the difference between the exact and approximate solutions is less dramatic at low velocities.

### Summary and conclusions

An exact solution for the one-dimensional heat transfer problem in the microslide of a directional solidification stage has been presented in this study. Results of this study indicate that the cooling-rate distribution along the microslide is by no means uniform. At lower microslide velocities of less than 25 µm s<sup>-1</sup>, the cooling-rates are within the range 95% to 110% of those calculated by the commonly accepted approximate solution. At microslide velocities of the order of 10<sup>2</sup> µm s<sup>-1</sup>, the cooling-rate can vary by several hundred percent along the microslide.

Regardless of the microslide velocity, the cooling-rates at the initiation of the microslide movement are significantly higher than those at steady-state. The time period required for this initiation effect to disappear is also addressed in this report. For practical cases, the microslide heat transfer may be assumed to reach steady-state for Fourier values greater than 1.8.

The exact solution should serve as an engineering tool for thermal design of the directional solidification stage, and especially for high velocities. For example, there is no sense in trying to obtain higher certainty in base temperature

distribution than the certainty in evaluating the temperature at the point of microscopic observations.

Finally, a constant cooling-rate, within the high cooling-rate part of the spectrum, can be achieved by applying a varying microslide velocity. In this case, the pre-specified cooling-rate relates to a pre-specified location on the microslide, and the heat transfer problem should be solved numerically.

### Acknowledgement

The author would like to thank Mrs Miriam Webber for her assistance in preparing this paper.

### References

- Brower, W.E., Freund, M.J., Baudino, M.D. & Ringwald, C. (1981) An hypothesis for survival of spermatozoa via encapsulation during plane front freezing. *Cryobiology*, **18**, 277–291.
- Carnahan, B., Luther, H.A. & Wilkes, J.O. (1969) *Applied Numerical Methods*. Wiley, New York.
- Carslaw, H.S. & Jaeger, J.C. (1959) *Conduction of Heat in Solids*. Clarendon Press, Oxford.
- Cosman, M.D., Toner, M., Kandel, J. & Cravalho, E.G. (1989) An integrated cryomicroscopy system. *Cryo-Lett.* **10**, 17–38.
- Diller, K.R. (1982) A quantitative low temperature optical microscopy of biological systems. *J. Microsc.* **126**, 9–28.
- Diller, K.R. & Cravalho, E.G. (1971) A microscope for the study of freezing and thawing processes in biological cells. *Cryobiology*, **7**, 191–199.
- Korber, C.H., Scheiwe, M.W. & Wollhover, K. (1983) Solute polarization during planar freezing of aqueous solutions. *J. Heat Mass Trans.* **26**, 1241–1253.
- Luyet, B. & Rapatz, G. (1957) An automatically regulated refrigeration system for small laboratory equipment and a microscope cooling stage. *Biodynamica*, **7** (154), 337–345.
- Namperumal, R. & Cogger, R. (1998) A new cryostage design for microscopy. *J. Microsc.* **192**, 202–211.
- Rubinsky, B., Clayton, L. & Chaw, M. (1993) Experimental observations and theoretical studies on solidification processes in saline solutions. *Exp. Thermal Fluid Sci.* **6**, 157–167.
- Rubinsky, B. & Ikeda, M. (1985) A microscope using directional solidification for the controlled freezing of biological material. *Cryobiology*, **22**, 55–68.
- Tatsutani, K. & Rubinsky, B. (1998) A method to study intracellular ice nucleation. *ASME J. Biomech. Eng.* **120**, 27–31.